

# Study of solar and other unknown anti-neutrino fluxes with Borexino at LNGS

G. Bellini<sup>i,1</sup>, J. Benziger<sup>n</sup>, S. Bonetti<sup>i</sup>, M. Buizza Avanzini<sup>i</sup>, B. Caccianiga<sup>i</sup>, L. Cadonati<sup>p</sup>, F. Calaprice<sup>m</sup>, C. Carraro<sup>c</sup>, A. Chavarria<sup>m</sup>, A. Chepurinov<sup>j</sup>, D. D'Angelo<sup>i</sup>, S. Davini<sup>c</sup>, A. Derbin<sup>o</sup>, A. Etenko<sup>g</sup>, K. Fomenko<sup>b,h</sup>, D. Franco<sup>i</sup>, C. Galbiati<sup>m,2</sup>, S. Gazzana<sup>h</sup>, C. Ghiano<sup>h</sup>, M. Giammarchi<sup>i</sup>, M. Goeger-Neff<sup>k</sup>, A. Goretti<sup>m</sup>, E. Guardincerri<sup>c</sup>, S. Hardy<sup>q</sup>, Aldo Ianni<sup>h</sup>, Andrea Ianni<sup>m</sup>, M. Joyce<sup>q</sup>, V.V. Kobychiev<sup>e</sup>, D. Korablev<sup>b</sup>, Y. Koshio<sup>h</sup>, G. Korga<sup>h</sup>, D. Kryn<sup>a</sup>, M. Laubenstein<sup>h</sup>, M. Leung<sup>m</sup>, T. Lewke<sup>k</sup>, E. Litvinovich<sup>g</sup>, B. Loer<sup>m</sup>, P. Lombardi<sup>i</sup>, L. Ludhova<sup>i</sup>, I. Machulin<sup>g</sup>, S. Manecki<sup>q</sup>, W. Maneschg<sup>d</sup>, G. Manuzio<sup>c</sup>, Q. Meindl<sup>k</sup>, E. Meroni<sup>i</sup>, L. Miramonti<sup>i</sup>, M. Misiasek<sup>f</sup>, D. Montanari<sup>h,m</sup>, V. Muratova<sup>o</sup>, L. Oberauer<sup>k</sup>, M. Obolensky<sup>a</sup>, F. Ortica<sup>l</sup>, M. Pallavicini<sup>c</sup>, L. Papp<sup>h</sup>, L. Perasso<sup>i</sup>, S. Perasso<sup>c</sup>, A. Pocar<sup>p</sup>, R.S. Raghavan<sup>q</sup>, G. Ranucci<sup>i</sup>, A. Razeto<sup>h</sup>, A. Re<sup>i</sup>, P. Risso<sup>c</sup>, A. Romani<sup>l</sup>, D. Rountree<sup>q</sup>, A. Sabelnikov<sup>g</sup>, R. Saldanha<sup>m</sup>, C. Salvo<sup>c</sup>, S. Schönert<sup>d</sup>, H. Simgen<sup>d</sup>, M. Skorokhvatov<sup>g</sup>, O. Smirnov<sup>b</sup>, A. Sotnikov<sup>b</sup>, S. Sukhotin<sup>g</sup>, Y. Suvorov<sup>h</sup>, R. Tartaglia<sup>h</sup>, G. Testera<sup>c</sup>, D. Vignaud<sup>a</sup>, R.B. Vogelaar<sup>q</sup>, F. von Feilitzsch<sup>k</sup>, J. Winter<sup>k</sup>, M. Wojcik<sup>f</sup>, A. Wright<sup>m</sup>, M. Wurm<sup>k</sup>, J. Xu<sup>m</sup>, O. Zaimidoroga<sup>b</sup>, S. Zavatarelli<sup>c</sup>, G. Zuzel<sup>d</sup>,  
(Borexino Collaboration)

<sup>a</sup>Laboratoire AstroParticule et Cosmologie, 75231 Paris cedex 13, France

<sup>b</sup>Joint Institute for Nuclear Research, 141980 Dubna, Russia

<sup>c</sup>Dipartimento di Fisica, Università e INFN, Genova 16146, Italy

<sup>d</sup>Max-Planck-Institut für Kernphysik, 69029 Heidelberg, Germany

<sup>e</sup>Institute for Nuclear Research, 03680 Kiev, Ukraine

<sup>f</sup>M. Smoluchowski Institute of Physics, Jagiellonian University, 30059 Krakow, Poland

<sup>g</sup>RRC Kurchatov Institute, 123182 Moscow, Russia

<sup>h</sup>INFN Laboratori Nazionali del Gran Sasso, SS 17 bis Km 18+910, 67010 Assergi (AQ), Italy

<sup>i</sup>Dipartimento di Fisica, Università degli Studi e INFN, 20133 Milano, Italy

<sup>j</sup>Institute of Nuclear Physics, Lomonosov Moscow State University, 119899, Moscow, Russia

<sup>k</sup>Physik Department, Technische Universität Muenchen, 85747 Garching, Germany

<sup>l</sup>Dipartimento di Chimica, Università e INFN, 06123 Perugia, Italy

<sup>m</sup>Physics Department, Princeton University, Princeton, NJ 08544, USA

<sup>n</sup>Chemical Engineering Department, Princeton University, Princeton, NJ 08544, USA

<sup>o</sup>St. Petersburg Nuclear Physics Institute, 188350 Gatchina, Russia

<sup>p</sup>Physics Department, University of Massachusetts, Amherst, MA 01003, USA

<sup>q</sup>Physics Department, Virginia Polytechnic Institute and State University, Blacksburg, VA 24061, USA

---

## Abstract

We report on the search for anti-neutrinos of yet unknown origin with the Borexino detector at the Laboratori Nazionali del Gran Sasso. In particular, a hypothetical anti-neutrino flux from the Sun is investigated. Anti-neutrinos are detected through the neutron inverse  $\beta$  decay reaction in a large liquid organic scintillator target. We set a new upper limit for a hypothetical solar  $\bar{\nu}_e$  flux of  $760 \text{ cm}^{-2}\text{s}^{-1}$ , obtained assuming an undistorted solar  ${}^8\text{B}$  energy spectrum. This corresponds to a limit on the transition probability of solar neutrinos to anti-neutrinos of  $1.3 \times 10^{-4}$  (90% C.L.) for  $E_{\bar{\nu}} > 1.8 \text{ MeV}$ , covering the entire  ${}^8\text{B}$  spectrum. Best differential limits on anti-neutrino fluxes from unknown sources are also obtained between the detection energy threshold of 1.8 MeV and 17.8 MeV with more than 2 years of data.

*Keywords:* Anti-neutrinos, solar neutrinos, neutrino detector, liquid scintillator

---

1 The Borexino Collaboration has recently pub-

<sup>1</sup>spokesperson: Gianpaolo.Bellini@mi.infn.it

<sup>2</sup>Also at Fermi National Accelerator Laboratory, Batavia,

IL 60510, USA

lished a measurement of electron anti-neutrino fluxes at the Laboratori Nazionali del Gran Sasso (LNGS) [1]. Contributions from two known sources were observed: 1)  $\bar{\nu}_e$ 's produced in nuclear reactors and 2) geo-neutrinos, produced in  $\beta$  decays of isotopes along the decay chains of long-lived  $^{238}\text{U}$  and  $^{232}\text{Th}$  distributed within the Earth's interior. An  $\bar{\nu}_e$  rate of  $4.3^{+1.7}_{-1.4}$  events/(100 ton yr) was measured from nuclear reactors, consistent with an expected rate of  $5.7 \pm 0.3$  events/(100 ton yr). Geo-neutrinos were identified at a rate of  $3.9^{+1.6}_{-1.3}$  events/(100 ton yr).

In this letter we present a study of other possible anti-neutrino sources. These include the search for hypothetical solar anti-neutrinos and the investigation of other, unspecified and model-independent  $\bar{\nu}_e$  fluxes. A weak anti-neutrino flux from the Sun arising from  $\bar{\nu}_e \rightarrow \nu_e$  conversion cannot be completely excluded with current experimental data. In particular, the interplay of flavor oscillations and spin flavor precession (SFP) induced by solar magnetic fields on Majorana neutrinos with sizable electric or magnetic transition moments [2]-[14] could lead to the appearance of an  $\bar{\nu}_e$  admixture in the solar neutrino flux.

The current best limit on the solar anti-neutrino flux is  $\phi_{\bar{\nu}_e} < 370 \text{ cm}^{-2}\text{s}^{-1}$  (90% C.L.), reported by KamLAND [15]. The analysis was performed in the  $8.3 < E_{\bar{\nu}_e} < 14.8 \text{ MeV}$  energy range. Assuming the undistorted solar  $^8\text{B}$  spectrum, the limit on the anti-neutrino flux scaled to the entire energy range is  $\phi_{\bar{\nu}_e} < 1250 \text{ cm}^{-2}\text{s}^{-1}$  (90% C.L.), and a limit on the conversion probability  $p_{\nu \rightarrow \bar{\nu}} < 2.8 \times 10^{-4}$  (90% C.L.) was set using the  $^8\text{B}$  theoretical solar neutrino flux of  $5.05^{+0.20}_{-0.16} \times 10^6 \text{ cm}^{-2}\text{s}^{-1}$  [16]<sup>3</sup>. The expected background from known sources for this search in the energy range of interest was  $1.1 \pm 0.4$  events/(0.28 kt yr) and no candidate events were observed in 185 days of data taking.

Although a smaller detector than KamLAND, Borexino has a competitive sensitivity in the high energy portion of the anti-neutrino energy spectrum, above reactor anti-neutrinos. At lower energies, Borexino compensates its size disadvantage with a significantly lower anti-neutrino background, due to its large distance from nuclear power plants (the average baseline is  $\sim 1000 \text{ km}$ ) and with lower intrinsic radioactive background.

<sup>3</sup>In order to make the comparison of results clearer, we underline that the value for the  $^8\text{B}$  flux used in current work is  $5.88 \times 10^6 \text{ cm}^{-2}\text{s}^{-1}$  [17].

Borexino [18]-[20] is a large volume, unsegmented organic liquid scintillator detector located underground at the Laboratori Nazionali del Gran Sasso, Italy. Primarily designed for a real-time, high precision measurement of the mono-energetic (862 keV)  $^7\text{Be}$  solar neutrino flux via  $\nu - e$  elastic scattering interactions in the scintillator, Borexino is also an extremely sensitive anti-neutrino detector. It began data taking in May 2007 and has already presented a measurement of the  $^7\text{Be}$  solar neutrino flux with 10% precision [21]. Because both  $\beta$  and  $\gamma$  interactions are essentially indistinguishable from the sought-after neutrino induced events, the measurement was possible thanks to the high purity from radioactive contaminants achieved in the scintillator and surrounding detector components,  $(1.6 \pm 0.1) \times 10^{-17} \text{ g/g}$  for  $^{238}\text{U}$  and  $(6.8 \pm 1.3) \times 10^{-18} \text{ g/g}$  for  $^{232}\text{Th}$  [21].

A central spherical core of 278 tons (design value) of organic liquid scintillator (LS) solution, constituted of pseudocumene solvent (1,2,4-trimethylbenzene  $\text{C}_6\text{H}_3(\text{CH}_3)_3$ ) doped with PPO fluor (2,5-diphenyloxazole,  $\text{C}_{15}\text{H}_{11}\text{NO}$ ) with a concentration of 1.5 g/l, is contained within a 8.5 m-diameter thin transparent nylon vessel (Inner Vessel, IV) and viewed by 2212 large area 8" photomultiplier tubes (PMTs) defining the inner detector (ID) and providing 34% geometric coverage. The scintillator is immersed in  $\sim 1000$  tons of pseudocumene buffer fluid, divided into two regions by a second transparent nylon vessel 11.5 m in diameter, which prevents radon gas to permeate into the scintillator. Scintillator and buffer fluid are contained within a 13.7 m-diameter stainless steel sphere (SSS) on which the inward-looking PMTs are mounted. DMP (dimethylphtalate) dissolved in the buffer fluid quenches undesired scintillation from residual radioactivity contained in the SSS and PMTs. The SSS is immersed in a large water tank (WT) for further shielding from high energy  $\gamma$  rays and neutrons emerging from the surrounding rock. The WT is instrumented as a Čerenkov muon detector (outer detector, OD) with additional 208 PMTs, particularly important for detecting muons skimming the central detector inducing signals in the energy region of interest for neutrino physics. A detailed description of the Borexino detector can be found in Refs. [19, 20].

A high light yield of  $\simeq 500$  photoelectrons (p.e.) detected for every 1 MeV of electron energy deposited gives an energy resolution of  $\sim 5\%$  at 1 MeV. The position of each scintillation event in Borexino

is determined from the timing pattern of hit PMTs with a spatial reconstruction algorithm. The code has been tuned using data from several calibration campaigns with radioactive sources inserted at different positions inside the detector. A maximum deviation of 5 cm between the reference and reconstructed source positions is observed at a radius of  $\sim 4$  m, close to the bottom of the IV.

In Borexino, anti-neutrinos are detected via the neutron inverse  $\beta$  decay reaction,  $\bar{\nu}_e + p \rightarrow n + e^+$ , with a kinematic threshold  $E_{\bar{\nu}} > 1.8$  MeV. The cross section for this process is much higher than for  $\bar{\nu} - e$  elastic scattering, making it the dominant anti-neutrino interaction in proton-rich water-Čerenkov and liquid scintillator detectors. This process also offers an experimentally unique signature given by the close time sequence of correlated events. The positron promptly annihilates emitting two 511 keV  $\gamma$ -rays, providing the prompt event, with a visible energy of  $E_{\text{prompt}} = E_{\bar{\nu}} - 0.782$  MeV (the scintillation light related to the proton recoil is highly quenched and negligible). The neutron quickly thermalizes and is then captured by a proton after a time characteristic of the medium, via the reaction  $n + p \rightarrow d + \gamma$ . For protons, the de-excitation  $\gamma$  ray is 2.2 MeV and constitutes the delayed event. For the Borexino scintillator the mean capture time was measured to be  $\sim 256$   $\mu\text{s}$ . The coincident nature of anti-neutrino events allows for the detection of relatively few events with high significance. Incidentally, the 2.2 MeV photon is detected with low efficiency in water-Čerenkov detectors.

For the present analysis we used two antineutrino candidates selection criteria. With data set A, we selected anti-neutrinos candidates in the entire scintillator volume from the data collected between May 2007 and June 2010. The live time for set A after all analysis cuts is 736 days. Data set B coincides with the one used for the geo-neutrino analysis [1] and includes data taken between December 2007 and December 2009, for a total 482 days of live time. Analogously to what was done for the geo-neutrino analysis, a fiducial volume cut, detailed below, was introduced for data set B in order to suppress neutron background from  $^{13}\text{C}(\alpha, n)^{16}\text{O}$  reactions initiated by  $^{210}\text{Po}$   $\alpha$  decays in the non-scintillating buffer fluid surrounding the scintillator.

The following anti-neutrino candidates selection criteria have been defined based on calibration data and Monte Carlo (MC) simulations and applied to the data. All cuts apply to both data sets unless

otherwise noted.

1.  $Q_{\text{prompt}} > 410$  p.e.; for reference,  $Q = 438 \pm 2$  p.e. corresponds to the positron annihilation at rest with  $E = 1.022$  MeV released at the center of the detector.
2.  $700 < Q_{\text{delayed}} < 1250$  p.e.; 2.2 MeV  $\gamma$ 's deposit  $1060 \pm 5$  p.e. at the detector's center; the lower limit is justified because photons at the edge of the scintillator can escape depositing none or only a fraction of their total energy).
3.  $20 < \Delta T < 1280$   $\mu\text{s}$ , where  $\Delta T$  is the time between prompt and delayed event. The upper limit is 5 times the mean neutron capture time and guarantees good acceptance. The lower limit excludes double cluster events, *i.e.* events that fall within the same data acquisition gate, which present higher background contamination.
4. Reconstructed distance between prompt and delayed events:  $\Delta R < 1$  m for data set B,  $\Delta R < 1.5$  m for data set A to increase the acceptance.
5.  $R_{\text{prompt}} < R_{\text{IV}}(\theta, \phi) - 0.25$  m for data set B, where  $R_{\text{prompt}}$  is the reconstructed radius for the prompt event and  $R_{\text{IV}}(\theta, \phi)$  is the inner vessel radial size in the direction  $(\theta, \phi)$  of the event (the IV is not exactly spherical; its true shape is reconstructed using seven CCD cameras mounted on the SSS). No volume cut is applied for data set A.
6. All tagged muon events are dropped. Muons can cause events which mimic  $\bar{\nu}_e$  events as illustrated in [1]. Cosmic muons are typically identified by the OD, but can also be distinguished from point-like scintillation events by the pulse shape analysis of the ID signal. The probability to miss a muon after identification by the OD and pulse shape analysis is  $3 \times 10^{-5}$  [1].
7. A 2 ms veto is applied after each muon which crosses the outer but not the inner detector in order to suppress background from fast neutrons produced along their tracks in water.
8. A 2 second veto is applied after each muon crossing the inner detector to suppress the  $\beta$ - $n$  decaying cosmogenic isotopes  $^9\text{Li}$  ( $\tau = 260$  ms) and  $^8\text{He}$  ( $\tau = 173$  ms).

201 Approximately 4300 muons traverse the ID every 253  
 202 day, and an equivalent amount cross the OD alone. 254  
 203 Cuts 6 and 7 thus introduce a modest dead time. 255  
 204 Cut 8 corresponds to  $\sim 8600$  seconds of dead time 256  
 205 per day, or about 10%. A careful study of cuts 6-8 257  
 206 yielded a total dead time of 10.5%. The combined 258  
 207 acceptance  $\epsilon$  of all other cuts (1-5) is estimated by 259  
 208 MC means at  $(85 \pm 1)\%$  for data set B and  $(83 \pm 1)\%$  260  
 209 for data set A, mostly attributable to the  $\Delta T$  ( $\epsilon =$   
 210  $91.8\%$ ) and  $\Delta R$  ( $\epsilon \sim 95\%$ ) cuts, and partially due  
 211 to the loss of  $\gamma$  rays close to the IV surface.

212 The energy of each event is reconstructed using  
 213 the total amount of light registered by all PMTs of 261  
 214 the detector (measured in photoelectrons, p.e.) and 262  
 215 corrected with a position-dependent light collection 263  
 216 function  $f(x, y, z)$ , which relates the light yield at 264  
 217 point  $(x, y, z)$  to that of the same event at the 265  
 218 center of the detector,  $Q(x, y, z) = f(x, y, z) Q_0$ . 266  
 219 An extensive calibration campaign with a set of 267  
 220 gamma sources has been performed (the energy of 268  
 221 the gamma rays ranged between a few hundred keV 269  
 222 to 9 MeV). For events at the center of the detec- 270  
 223 tor, the total amount of light collected is linear 271  
 224 with energy above 1 MeV [22]. The  $f(x, y, z)$  func- 272  
 225 tion was constructed using calibration data from 273  
 226 sources deployed at different positions inside the 274  
 227 detector and checked against MC simulations. The 275  
 228 correction is up to 15% at the poles of the detec-  
 229 tor, where scintillation light is shadowed the most  
 230 by the conduits used to fill the detector. The es-  
 231 timated (systematic) uncertainty of the energy re-  
 232 construction procedure is about 2%. It is mainly 276  
 233 due to the uncertainty in the  $f(x, y, z)$  function, 277  
 234 with a small contribution from the stability of the 278  
 235 energy scale of the detector. The most energetic 279  
 236 anti-neutrino candidate event in the entire data set 280  
 237 has a total light yield  $Q_{\text{prompt}} = 2,996$  p.e. and 281  
 238 is located within the fiducial volume defined for 282  
 239 data set B.  $Q_{\text{prompt}} = 2996$  p.e. corresponds to 283  
 240  $Q_0 = 2991$  p.e. at the center of the detector, or 284  
 241  $E = 6.22 \pm 0.12$  (*syst*) MeV. We looked for an 285  
 242 admixture of anti-neutrinos within the solar neu- 286  
 243 trino flux, considering the case of energy indepen- 287  
 244 dent conversion. Data Set A was used for this anal- 288  
 245 ysis, with a threshold of 6.5 MeV for the visible 289  
 246 energy (corresponding to an anti-neutrino energy 290  
 247 of 7.3 MeV). With this threshold, the expected 291  
 248 background in Data Set A is mainly due to the high 292  
 249 energy tail of reactor anti-neutrinos, is estimated at 293  
 250  $N_R = 0.31 \pm 0.02$  events. Additional backgrounds 294  
 251 are hard to define and quantify, but in a conserva- 295  
 252 tive approach we can simply use the lowest possible 296

value, i.e. zero background. The absence of anti-  
 neutrino candidates in the entire  $270 \pm 3$  tons of  
 scintillator (as calculated by reconstructing the ex-  
 act shape of the IV by means of images taken with  
 seven inward-looking CCD cameras mounted on the  
 SSS) during an observation time of  $T = 736$  days is  
 then used to set the following limit on a hypothet-  
 ical solar anti-neutrino flux:

$$\phi_{\text{lim}} = \frac{S_{\text{lim}}}{\bar{\sigma} \cdot T \cdot N_p \cdot \epsilon} \text{ cm}^{-2} \text{ s}^{-1}, \quad (1)$$

where  $N_p = (1.62 \pm 0.02) \times 10^{31}$  is the number of  
 target protons,  $\bar{\sigma}$  is the average cross section for  
 neutron inverse beta decay [23] weighted over the  
 ${}^8\text{B}$  solar neutrino spectrum [24] in the energy range  
 of interest,  $S_{\text{lim}}$  is the maximum allowed signal at  
 90% C.L. and  $\epsilon = 0.83 \pm 0.01$  is the efficiency (con-  
 stant within the chosen interval) of inverse beta-  
 decay detection for the chosen set of selected cuts,  
 defined with MC simulation.

Assuming an undistorted solar  ${}^8\text{B}$  neutrino en-  
 ergy spectrum  $\bar{\sigma}(E_{\bar{\nu}} > 7.3) = 6.0 \times 10^{-42} \text{ cm}^2$  and  
 with  $S_{\text{lim}} = 2.13$ , obtained applying the Feldman-  
 Cousins procedure [25] for the case of no observed  
 events with 0.31 expected background events we ob-  
 tain:

$$\phi_{\bar{\nu}}({}^8\text{B}, E > 7.3 \text{ MeV}) < 415 \text{ cm}^{-2} \text{ s}^{-1} \text{ (90\% C.L.)}.$$

Part of the spectrum above 7.3 MeV corresponds to  
 42% of the total  ${}^8\text{B}$  neutrino spectrum [24], equiv-  
 alently  $\phi_{\bar{\nu}}({}^8\text{B}) < 990 \text{ cm}^{-2} \text{ s}^{-1}$  at 90% C.L. over  
 the entire  ${}^8\text{B}$  neutrino spectrum. This corresponds  
 to an average transition probability in this energy  
 range of  $p_{\nu \rightarrow \bar{\nu}} < 1.7 \times 10^{-4}$  obtained assuming  
 $\phi_{SSM}({}^8\text{B}) = 5.88 \times 10^6 \text{ cm}^{-2} \text{ s}^{-1}$  [17] (we do not  
 take into account the errors on the theoretical pre-  
 dictions of the  ${}^8\text{B}$  neutrino flux).

A limit was alternatively obtained using data  
 set B over the entire  ${}^8\text{B}$  spectrum. The reduced  
 statistics due to the lower target fiducial volume  
 ( $N_p = 1.34 \times 10^{31}$ ), shorter data taking period  
 ( $T = 482$  days) and lower acceptance on  $\Delta R$  with  
 respect to data set A is partially compensated by  
 the larger energy range and a higher detection ef-  
 ficiency,  $\epsilon = 0.85 \pm 0.01$ . Applying the fit pro-  
 cedure developed for the geo-neutrino studies [1]  
 and following the  $\chi^2$  profile as a function of the  
 amount of additional, hypothetical, anti-neutrinos  
 under the assumption of an energy-independent  ${}^8\text{B}$

297 solar neutrino conversion to anti-neutrino, we obtain  
 298  $S_{\text{lim}} = 2.90$  at 90% C.L. From (1) and with  
 299  $\bar{\sigma}(E_{\bar{\nu}} > 1.8) = 3.4 \times 10^{-42} \text{ cm}^2$ :

$$\phi_{\bar{\nu}}(^8\text{B}) < 1820 \text{ cm}^{-2}\text{s}^{-1} \text{ (90\% C.L.)}$$

300 or  $p_{\nu \rightarrow \bar{\nu}} < 3.1 \times 10^{-4}$  in the energy range above  
 301 1.8 MeV. This limit is weaker than that obtained  
 302 by simple scaling of the result from the study above  
 303 7.3 MeV.

The strongest limit was obtained combining both  
 data sets (below/above 7.3 MeV we used the data  
 sets B/A, respectively). We applied the fit pro-  
 cedure developed for the geo-neutrino studies [1]  
 with the  $^8\text{B}$  neutrino spectrum correctly weighted  
 for effective exposures below and above 7.3 MeV.  
 Following the  $\chi^2$  profile with respect to the amount  
 of additional hypothetical anti-neutrinos assuming  
 an energy-independent  $^8\text{B}$  neutrino conversion to  
 anti-neutrino, we obtain  $S_{\text{lim}} = 2.07$  at 90% C.L.  
 (the corresponding fraction above 7.3 MeV is 1.64).  
 Using (1) with  $\bar{\sigma} = 6.0 \times 10^{-42} \text{ cm}^2$

$$\phi_{\bar{\nu}}(^8\text{B}, E > 7.3\text{MeV}) < 320 \text{ cm}^{-2}\text{s}^{-1} \text{ (90\% C.L.,)}$$

which in the total energy range corresponds to:

$$\phi_{\bar{\nu}}(^8\text{B}) < 760 \text{ cm}^{-2}\text{s}^{-1} \text{ 90\% C.L.,}$$

304 or  $p_{\nu \rightarrow \bar{\nu}} < 1.3 \times 10^{-4}$  for the total  $^8\text{B}$  flux. This  
 305 limit is stronger than that obtained by simple scal-  
 306 ing of the result from the study above 7.3 MeV  
 307 energy range. Our limits for  $\bar{\nu}$  flux with undis-  
 308 torted solar  $^8\text{B}$  neutrino spectrum are summarized  
 309 in Tab. 1, where they are compared with those re-  
 310 ported by SuperKamiokaNDE [26], KamLAND [15]  
 311 and SNO [27]. The upper limit on a hypothet-  
 312 ical solar anti-neutrino rate is illustrated against  
 313 the Borexino measured reactor and geo-neutrino  
 314 rates [1] in Fig. 1.

315 The limit on solar anti-neutrinos allows us to set  
 316 limits on the neutrino magnetic moment  $\mu_{\nu}$  and  
 317 on the strength and shape of the solar magnetic  
 318 field. Assuming the SFP mechanism coupled with  
 319 the MSW-LMA solar neutrino solution, limits on  
 320 the neutrino magnetic moment  $\mu_{\nu}$  can be obtained  
 321 using the limits on the conversion probability  $p_{\nu \rightarrow \bar{\nu}}$ ,  
 322 as shown in [8, 9, 10]. In general, the limit on  $\mu_{\nu}$   
 323 depends on the unknown strength of the solar mag-  
 324 netic field  $B$  in the neutrino production region, and  
 325 can be written as [8]:

$$\mu_{\bar{\nu}} \leq 7.4 \times 10^{-7} \left( \frac{p_{\nu \rightarrow \bar{\nu}}}{\sin^2 2\theta_{12}} \right)^{1/2} \frac{\mu_B}{B_{\perp} [\text{kG}]}$$

326 where  $\mu_B$  is Bohr's magneton and  $B_{\perp}$  is the trans-  
 327 verse component of the solar magnetic field at a ra-  
 328 dius  $0.05R_{\odot}$  corresponding to the maximum of  $^8\text{B}$ -  
 329 neutrino production. Using our experimental limit  
 330  $p_{\nu \rightarrow \bar{\nu}} = 1.3 \times 10^{-4}$  and  $\sin^2 2\theta_{12} = 0.86$  [28, 29]  
 331 one obtains  $\mu_{\nu} \leq 9 \times 10^{-9} B_{\perp} \mu_B$  (90% C.L.).  
 332 Solar physics provides very limited knowledge on  
 333 magnitude and shape of solar magnetic fields. In  
 334 accordance with [30, 31, 32] the magnetic field  
 335 in the core can vary between 600 G and 7 MG.  
 336 The higher value limits the magnetic moment to  
 337  $\mu_{\nu} \leq 1.4 \times 10^{-12} \mu_B$ .

The spin flip could also occur in the convective  
 zone of the Sun in which neutrinos traverse a region  
 of random turbulent magnetic fields [11, 12, 13].  
 Using the expression for the conversion probabili-  
 ty given in [13, 33] and the solar neutrino mix-  
 ing parameters  $\cos^2 \theta_{12} = 0.688$  and  $\Delta m^2 = 7.64 \times$   
 $10^{-5} \text{ eV}^2$  [28, 29], the limit on the magnetic moment  
 can be written as:

$$\mu_{\bar{\nu}} \leq 8.2 \times 10^{-8} p_{\nu \rightarrow \bar{\nu}}^{1/2} B^{-1} [\text{kG}] \mu_B$$

338 where  $B$  is the average strength of the turbulent  
 339 magnetic field. Using conservative values for  $B$  of  
 340 10-20 kG [12, 13, 33, 34], we obtain less stringent  
 341 limits on the magnetic moment than current labora-  
 342 tory bounds.

343 Currently, the best limit on the neutrino mag-  
 344 netic moment,  $\mu_{\nu} < 3 \times 10^{-12} \mu_B$ , is obtained by  
 345 imposing astrophysical constraints that avoid ex-  
 346 cessive energy losses by globular-cluster stars [35].  
 347 The best direct limit is obtained with reactor neu-  
 348 trinos,  $\mu_{\bar{\nu}_e} < 3.2 \times 10^{-11} \mu_B$  [36] or  $\mu_{\bar{\nu}_e} < 5 \times 10^{-12}$   
 349  $\mu_B$  when atomic ionization is taken into account  
 350 [37]. The best limit on the effective magnetic mo-  
 351 ment of solar neutrinos is close,  $\mu_{\nu} < 5.4 \times 10^{-11}$   
 352 (90% C.L.) [21]. It was obtained by the Borex-  
 353 ino Collaboration by studying the shape of the  
 354 electron recoil energy spectrum following elastic  
 355 scattering from mono-energetic  $^7\text{Be}$  solar neutri-  
 356 nos. These experimental limits on the neutrino  
 357 magnetic moments, together with reasonable as-  
 358 sumptions on the distribution of turbulent magnetic  
 359 fields in the Sun, corresponds to a conversion proba-  
 360 bility  $p_{\nu \rightarrow \bar{\nu}} \sim 10^{-6}$ , about two orders of magnitude  
 361 lower than the sensitivity of present experiments.

362 The case of an undistorted  $^8\text{B}$  antineutrino spec-  
 363 trum is a special case of  $\nu \rightarrow \bar{\nu}$  conversion. For the  
 364 more general case, a model-independent search for  
 365 unknown anti-neutrino fluxes was performed in 1  
 366 MeV energy bins for  $1.8 \text{ MeV} < E_{\bar{\nu}} < 17.8 \text{ MeV}$ .

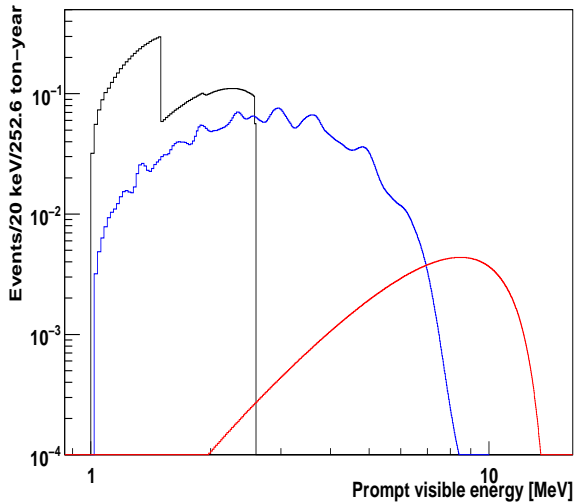


Figure 1: Energy spectra for electron anti-neutrinos in Borexino. The horizontal axis shows the kinetic plus the annihilation 1.022 MeV energy of the prompt positron event. Shown are expected shapes for geo- (black line) and reactor (blue line) anti-neutrinos normalized to the Borexino measured values [1] for a 252.6 ton year exposure. Effects of neutrino oscillations are included. The spectral shape for hypothetical  ${}^8\text{B}$  solar anti-neutrinos is shown in red and normalized to our upper limit of  $1.3 \times 10^{-4} \phi_{SSM}({}^8\text{B})$  (see text for details)

This study was made possible by the extremely low background achieved by Borexino. The analysis consisted in setting the limits on any contribution of unknown origin in the antineutrino spectrum registered by Borexino. Data set B was used below 7.8 MeV (same region used in our recent study of geo-neutrinos), where reactor and geo-neutrinos positively contribute to the signal, with 21 detected candidate events within 225.1 tons of scintillator during 482 days of data taking and an average detection efficiency  $\epsilon = 0.85$  [1]. Data set A was used above 7.8 MeV where, as mentioned earlier, no events were recorded allowing us to use the full scintillator volume and a more inclusive  $\Delta R$  value between the prompt and delayed events. The live time was 736 days with an average detection efficiency  $\epsilon = 0.83$ . Decrease in the detection efficiency at high energies due to muon software tagging over-efficiency via ID pulse shape analysis was considered and evaluated by MC simulations. The robustness of the event binning was tested against the precision of the light yield-to-energy conversion, which carries a 2% systematic uncertainty as mentioned earlier.

Table 1: Limits on the  $\bar{\nu}$  flux with undistorted  ${}^8\text{B}$  spectrum for the Borexino, its prototype CTF, KamLAND, SNO and SuperKamiokaNDE experiments. Upper limits are given at 90% C.L. (see text for details).

Experiment	Measurement threshold [MeV]	Total $\phi_{\bar{\nu}_e}({}^8\text{B})$ 90% C.L. [ $\text{cm}^{-2}\text{s}^{-1}$ ]
CTF [38]	$> 1.8$	$< 1.1 \times 10^5$
SNO [27]	$> 4$	$< 4.09 \times 10^4$
SuperK [26]	$> 8$	$< 4.04 \times 10^4$
KamLAND [15]	$> 8.3$	$< 1250$
Borexino (this work)	$> 7.3$	$< 990$
Borexino (this work)	$> 1.8$	$< 760$

The number of events assigned to each bin is not sensitive to the variation of parameters (within 90% C.L.) with the exception of bins 2 and 3. One event happens to be on the boundary of these two bins (within  $\simeq 0.5\%$  energy interval) and we conservatively assigned it to both in setting our limits.

In order to have conservative limits, the minimal expected number of events in every bin has been calculated separately for reactor and geo-neutrinos. For geo-neutrinos we considered the Minimal Radiogenic Earth model [39], which only includes the radioactivity from U and Th in the Earth crust which can be directly measured in rock-samples. More details on the calculation can be found in Ref. [1].

The 90% C.L. upper limits  $S_{\text{lim}}$  in the Feldman-Cousins approach for the first eight bins are  $\{11.5, 6.48, 1.32, 4.93, 3.12, 3.96, 2.38, 2.43\}$ , respectively. Above bin number 7 ( $E > 7.8$  MeV)  $S_{\text{lim}} = 2.44$ , obtained with the Feldman-Cousins recipe for no observed events with zero background. Model independent limits on anti-neutrino fluxes are illustrated in Fig. 2 and compared with SuperKamiokaNDE [26] and SNO [27] data.

As far as concerned the possible conversion of the low energy neutrino below the 1.8 MeV inverse beta decay reaction threshold, including those that could originate by SFP conversion of the abundant  ${}^7\text{Be}$  monoenergetic solar neutrinos, the only available detection channel is the elastic scattering on electrons. The recoil spectra for electrons elastically scattering off neutrino and anti-neutrinos are distinct, and we exploited such difference to search for an anti-neutrino admixture in the  ${}^7\text{Be}$  solar neu-

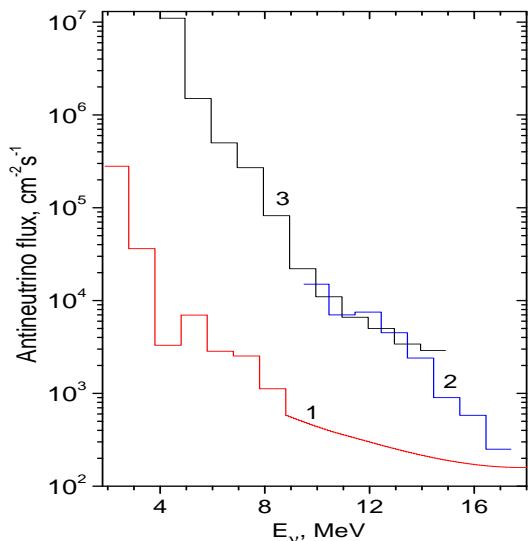


Figure 2: Upper limits on the monochromatic  $\bar{\nu}_e$  fluxes for: 1- the present Borexino data (red line); 2- SuperKamiokaNDE (blue line) [26] and 3- SNO (black line) [27]. The regions above the lines are excluded. The x-axis is anti-neutrino energy.

trino flux. Possible deviations from the pure  $\nu - e$  electron recoil shape due to electromagnetic interactions were studied in Borexino previously published data [21]. Following the changes in the  $\chi^2$  profile with respect to the addition of an anti-neutrino component we set a limit on the conversion probability for  ${}^7\text{Be}$  solar neutrinos of  $p_{\nu_e \rightarrow \bar{\nu}_e} < 0.35$  at 90% C.L. The relatively low sensitivity is in large part due to the strong anticorrelation between the  $\bar{\nu} - e$  elastic scattering spectrum and that of  ${}^{85}\text{Kr}$  (a  $\beta$  emitter which represents a significant residual background in Borexino) both left free in the analysis. It is likely that this limit could be improved following a purification campaign of the scintillator.

In conclusion, Borexino has shown excellent sensitivity to naturally-produced anti-neutrinos over a broad range of energies, thanks to its unprecedented radiological purity and its location far away from nuclear reactors. New limits have been set on the possible  $\bar{\nu}$  admixture in the solar neutrino flux. In particular,  $p_{\nu \rightarrow \bar{\nu}} < 1.7 \times 10^{-4}$  (90% C.L.) for  $E_{\bar{\nu}} > 7.3$  MeV,  $p_{\nu \rightarrow \bar{\nu}} < 1.3 \times 10^{-4}$  (90% C.L.) for the whole  ${}^8\text{B}$  energy region, and  $p_{\nu_e \rightarrow \bar{\nu}_e} < 0.35$  (90% C.L.) for 862 keV  ${}^7\text{Be}$  neutrinos. The best dif-

ferential limits on anti-neutrino fluxes of unknown origin between 1.8 and 17.8 MeV have also been set.

## 1. Acknowledgements

This work was funded by INFN (Italy), NSF (US Grant NSFPHY-0802646), BMBF (Germany), DFG (Germany, Grant OB160/1-1 and Cluster of Excellence Origin and Structure of the Universe), MPG (Germany), Rosnauka (Russia, RFBR Grant 09-02-92430), and MNiSW (Poland). This work was partially supported by PRIN 2007 protocol 2007 JR4STW from MIUR (Italy). O.Smirnov, L.Ludhova and A. Derbin acknowledge the support of Fondazione Cariplo.

## References

- [1] G. Bellini et al., Borexino Collaboration, Phys. Lett. B 687 (2010) 299.
- [2] J. Schechter and J.W.F. Valle, Phys. Rev. D 24 (1981) 1883 [Erratum ibid. D 25, 283 (1982)].
- [3] E.K. Akhmedov, Phys. Lett. B 213 (1988) 64.
- [4] C.S. Lim and W.J. Marciano, Phys. Rev. D 37 (1988) 1368.
- [5] R.S. Raghavan et al., Phys. Rev. D 44 (1991) 3786.
- [6] E.K. Akhmedov and J. Pulido, Phys. Lett. B 529 (2002) 193.
- [7] J. Barranco et al., Phys. Rev. D 66 (2002) 093009.
- [8] E.Kh. Akhmedov and J. Pulido, Phys. Lett. B 553 (2003) 7.
- [9] B.C. Chauhan, J. Pulido and E. Torrente-Lujan, Phys. Rev. D 68 (2003) 033015.
- [10] A.B. Balantekin and C. Volpe, Phys. Rev. D 72 (2005) 033008.
- [11] O.G. Miranda, T.I. Rashba, A.I. Rez and J.W.F. Valle, Phys. Rev. Lett. 93 (2004) 051304.
- [12] O.G. Miranda, T.I. Rashba, A.I. Rez and J.W.F. Valle, Phys. Rev. D 70 (2004) 113002.
- [13] A. Friedland, arXiv:hep-ph/0505165 (2005).
- [14] C. Giunti and A. Studenikin, Phys. Atom. Nucl. 72 (2009) 2089. (or arXiv:0812.3646v5 [hep-ph])
- [15] K. Eguchi et al. KamLAND Collaboration, Phys. Rev. Lett. 92 (2004) 071301.
- [16] J.N. Bahcall et al., Astrophys. J., 555 (2001) 990.
- [17] A.M. Serenelli, arXiv:0910.3690 (2009).
- [18] G. Alimonti, et al. Borexino Collaboration, Astropart. Phys. 16 (2002) 205.
- [19] G. Alimonti, et al. Borexino Collaboration, Nucl. Instr. and Methods A 600 (2009) 568.
- [20] G. Alimonti, et al. Borexino Collaboration, Nucl. Instr. and Methods A 609 (2009) 59.
- [21] C. Arpesella et al., Borexino Collaboration, Phys. Rev. Lett. 101(2008) 091302.
- [22] G. Bellini, et al., Borexino Collaboration, Phys. Rev. C 81 (2010) 034317.
- [23] A. Strumia and F. Vissani, Phys. Lett. B 564 (2003) 42.
- [24] J.N. Bahcall et al., Phys. Rev. C. 54 (1996) 411.
- [25] G.J. Feldman and R.D. Cousins, Phys. Rev. D 57 (1998) 3873.

- 504 [26] Y. Gando et al., SuperKamiokaNDE Collaboration,  
505 Phys. Rev. Lett. 90 (2003) 171302.
- 506 [27] B. Aharmim et al., SNO Collaboration, Phys. Rev. D  
507 70 (2004) 093014.
- 508 [28] G.L. Fogli et al., Phys. Rev. D 78 (2008) 033010.
- 509 [29] M.C. Gonzalez-Garcia, M. Maltoni and J. Salvado,  
510 JHEP 1005(2010) 072. arXiv:0910.4584v3
- 511 [30] L.L. Kitchatinov, Astron. Rep., 52 (2008) 247.
- 512 [31] A. Friedland and A. Gruzinov, Astrophys. J. 601 (2004)  
513 570.
- 514 [32] H.M. Antia, J. Astrophys. Astr. 29 (2008) 85.
- 515 [33] G. Raffelt and T. Rashba, Phys. Atom. Nucl. 73 (2010)  
516 609. (or arXiv:0902.4832v1 [astro-ph.HE])
- 517 [34] A. Friedland and A. Gruzinov, Astropart. Phys. 19  
518 (2003) 575.
- 519 [35] G. Raffelt and A. Weiss, Astron. Astrophys. 264 (1992)  
520 536.
- 521 [36] A.G. Beda, et al., arXiv:1005.2736 (2010).
- 522 [37] H.T. Wong, H.-B. Li and S.-T. Lin, Phys. Rev. Lett.  
523 105 (2010) 061801.
- 524 [38] M. Balata et al., Eur. Phys. J. C 47 (2006) 21.
- 525 [39] F. Mantovani, L. Carmignani, G. Fiorentini, M. Lissia,  
526 Phys. Rev. D 69 (2004) 013001.